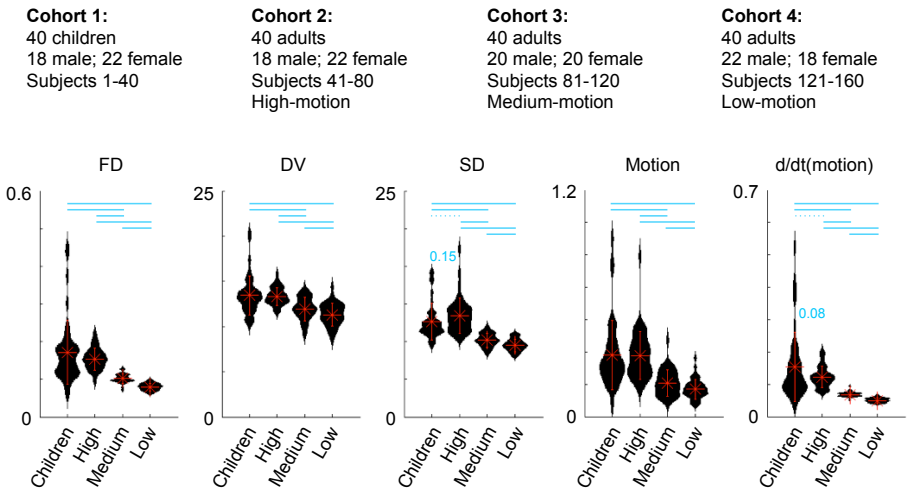

	1-2	1-3	1-4	2-3	2-4	3-4
Age	0.00	0.00	0.00	0.73	0.60	0.83
Volumes	0.84	0.09	0.51	0.02	0.31	0.24
FD	0.21	0.00	0.00	0.00	0.00	0.00
DV	0.76	0.00	0.00	0.00	0.00	0.03
SD	0.15	0.00	0.00	0.00	0.00	0.00
MVM	0.91	0.00	0.00	0.00	0.00	0.02
d/dt MVM	0.08	0.00	0.00	0.00	0.00	0.00

Children-High
Children-Medium
Children-Low
High-Medium
High-Low
Medium-Low

Figure S1: Cohort properties. At top, the sex composition and subject numbers of the 4 cohorts. The adult cohorts were formed by sorting a larger pool of 120 adult subjects by mean FD value and selecting the top 40, middle 40, and 40 lowest mean FD subjects with slight adjustment to achieve sex balance. Cohort properties, in terms of summary QC measures, are shown by violin plots, where the red star indicates the mean and the vertical red arms are standard deviations. Mean DV and SD were calculated before functional connectivity processing on data that were only demeaned and detrended, within the whole-brain mask. Cohort properties were compared using two-sample two-tailed t-tests; solid blue bars represent significant differences and dotted blue bars with blue numbers report trend-level p values (p values shown at right). The children and high-motion adult cohorts are not significantly different in any summary measure. These two high-motion cohorts differed from the medium- and low-motion adult cohort on all QC measures.

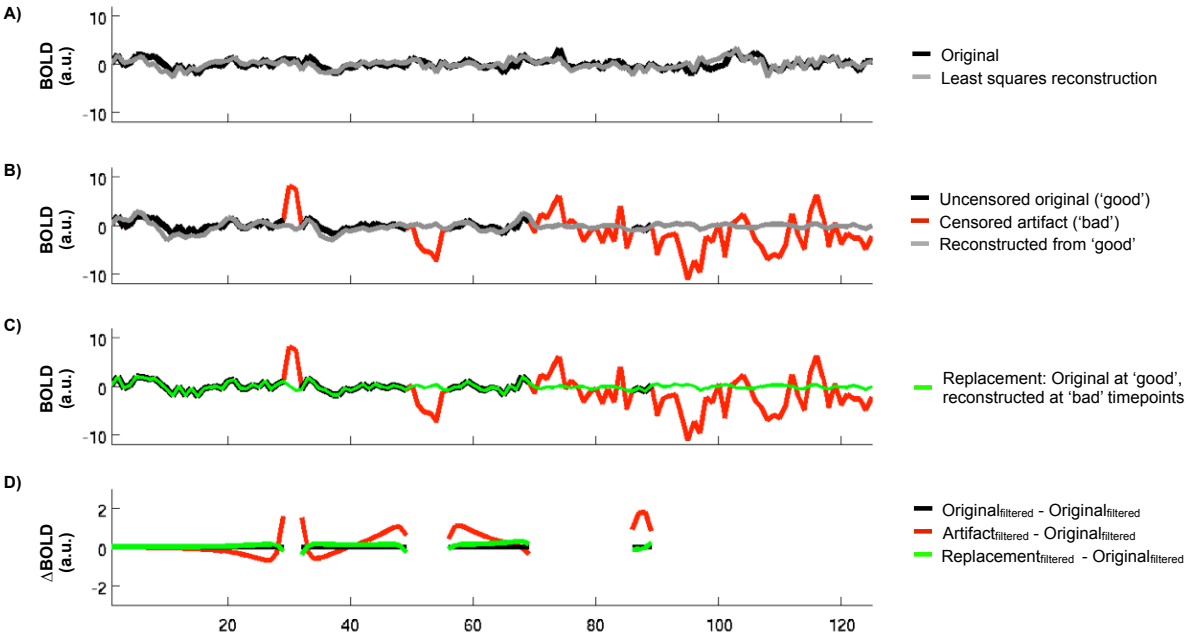

Figure S2: Replacing problematic data. This slide illustrates the method of interpolation used in this paper, using synthetic timeseries. **A)** In black, a synthetic timeseries of 125 timepoints with TR = 2.5 s. The gray trace is the least squares spectral reconstruction. **B)** Artifact, in red, has been added to the original timeseries at particular timepoints. The red artifactual trace is generated like the original, multiplied by 3, and added to the original timeseries. The gray trace is the reconstruction from the non-artifact-laden (uncensored) timepoints, analagous to the reconstruction used in the paper. **C)** The green trace illustrates the timeseries that would undergo temporal filtering in this paper: the original uncensored timeseries, with replacement at censored timepoints using the reconstructed timeseries generated from uncensored data. **D)** The differences after frequency filtering between the artifactual and original timeseries, and the interpolated and original timeseries. Only uncensored timepoints are shown (the data that would go into calculations). The deviation from the 'true' timeseries is greater for the red than the green trace, as expected, because interpolation reduces the amplitude of artifactual signal spread into adjacent timepoints during frequency filtering.

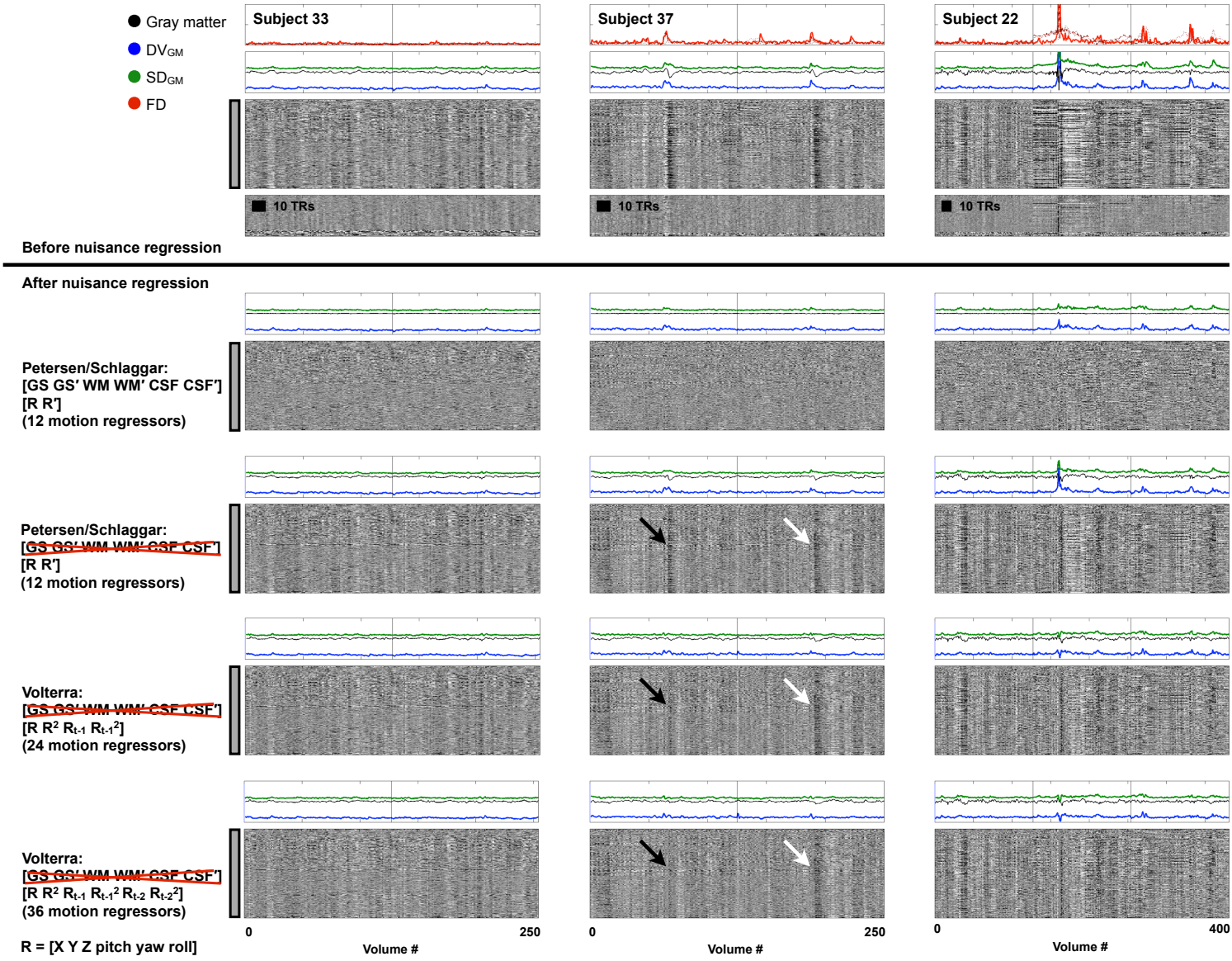
Gray matter
DVGM
SDGM
FD
Subject 33
Subject 37
Subject 22
10 TRs
10 TRs
10 TRs
Before nuisance regression
After nuisance regression
Petersen/Schlaggar:
[GS GS′ WM WM′ CSF CSF′]
[R R′]
(12 motion regressors)
Petersen/Schlaggar:
[GS GS′ WM WM′ CSF CSF′]
[R R′]
(12 motion regressors)
Volterra:
[GS GS′ WM WM′ CSF CSF′]
[R R2 Rt-1 Rt-12]
(24 motion regressors)
Volterra:
[GS GS′ WM WM′ CSF CSF′]
[R R2 Rt-1 Rt-12 Rt-2 Rt-22]
(36 motion regressors)
R = [X Y Z pitch yaw roll]
0
250
Volume #
0
250
Volume #
0
400
Volume #

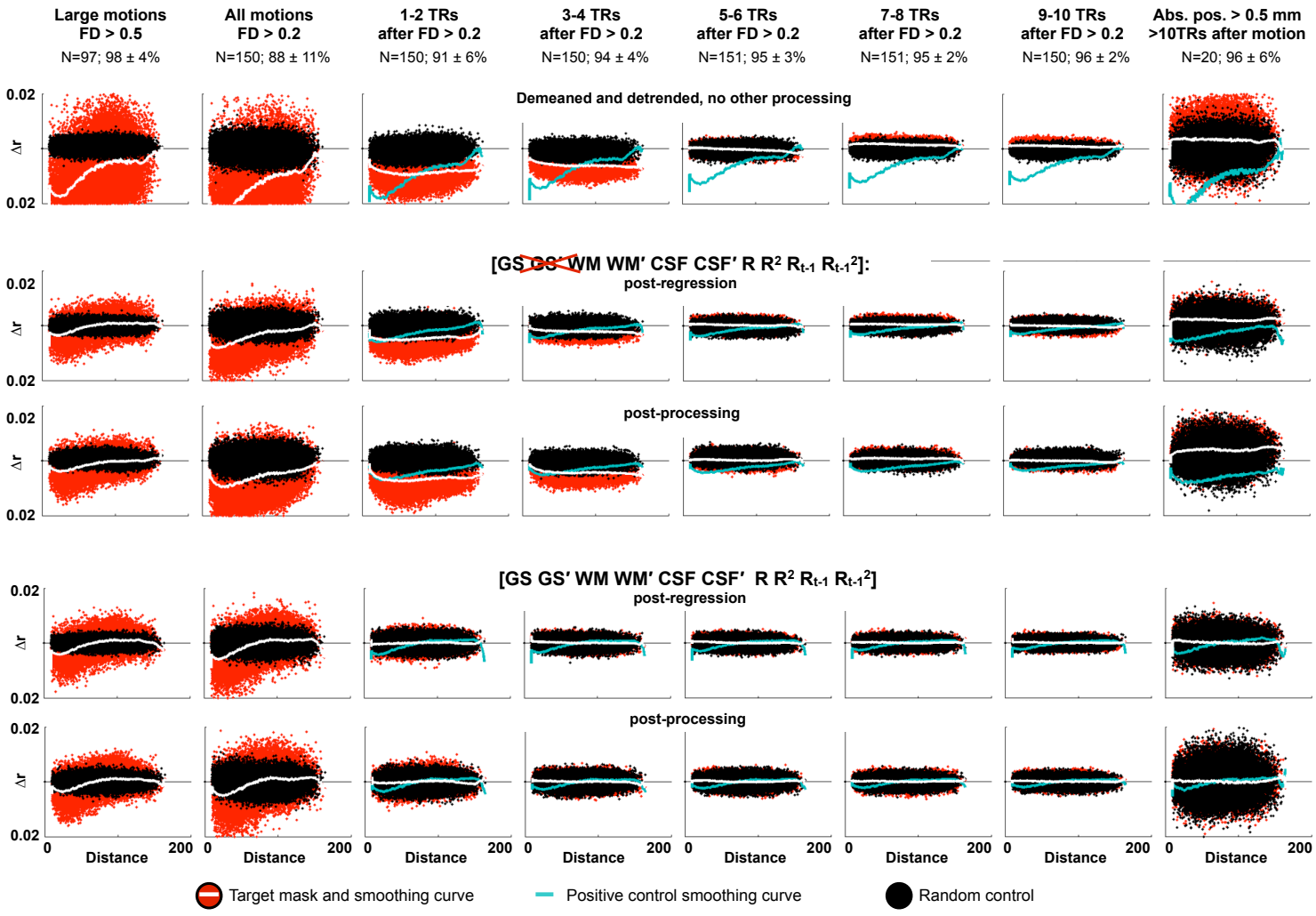

Figure S4: Analyses after Figure 8 for various stages of processing. These analyses extend the analyses in Figure 8 to later post-motion timepoints and to absolute head displacement. At top, data that are only demeaned and detrended are examined. Below, post-regression and fully processed timeseries are examined without and with GSR. The final mask (at right) isolates volumes where either absolute rotational or translational displacement was > 0.5 mm, and where no volumes with FD > 0.2 mm were present within the previous 10 volumes, thus isolating large head displacements from effects of motion.

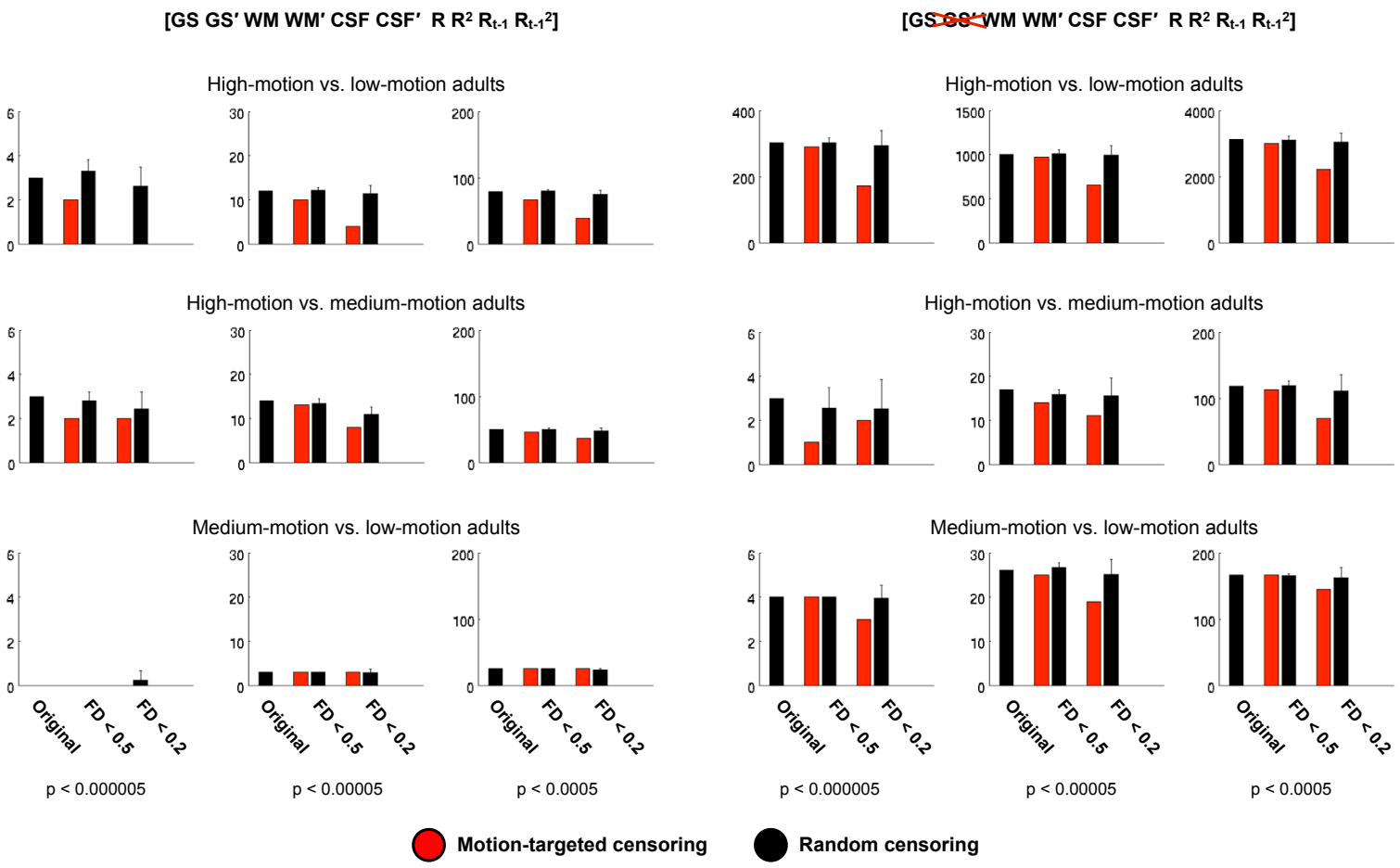

Figure S5: Plots after Figure 9 showing the selective decreases in group differences produced by motion-targeted scrubbing (red) compared to random scrubbing (black). Results from 3 statistical thresholds are shown. Error bars are standard deviations from 30 random repetitions.

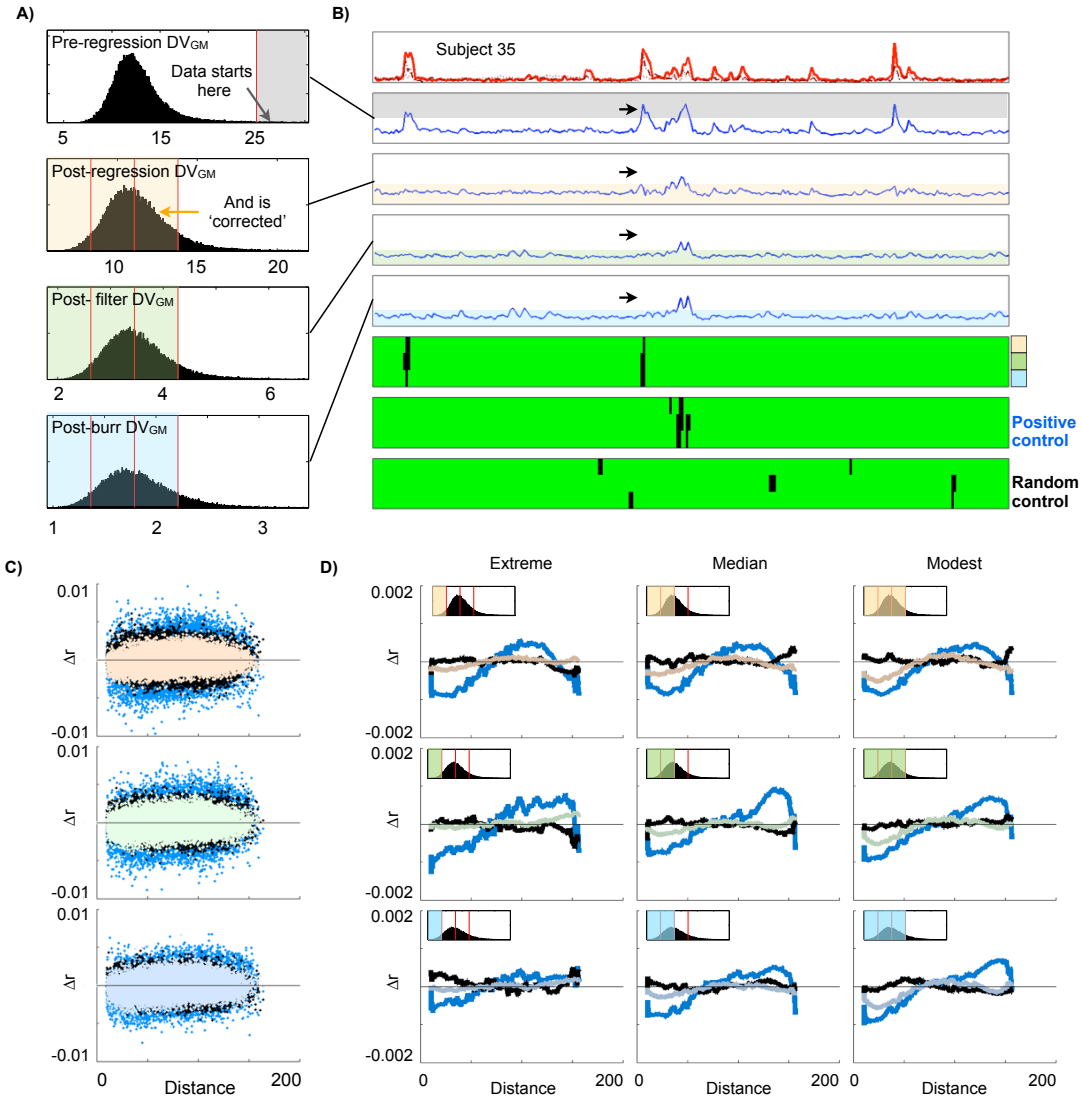

Figure S6: Reduced values of DV in later stages of processing do not reflect complete data correction and are partially cosmetic. A) The distributions of DV across all subject at different processing steps. Outlying initial values are shaded in gray. DV values below 1 standard deviation above the median are shaded in pastels. **B)** An example of the shaded regions in a single subject's DV traces, with an arrow indicating the type of volume under investigation. The target temporal masks identify volumes that begin with DV values in the gray shading but later have DV values in the pastel shadings. Positive control masks target high-DV volumes, and negative control masks are randomly targeted. **C)** Across all subjects who have data identified for censoring, the Δr produced by the masks shown in (A) and (B). **D)** Smoothing curves for each of the masks are shown. The 'modestly corrected' data in (A-C) are at far right, whereas the data in the middle show 'median corrected' volumes reduced to sub-median DV values, and the data at left show 'extremely corrected' volumes reduced to DV values more than 1 standard deviation below the median.

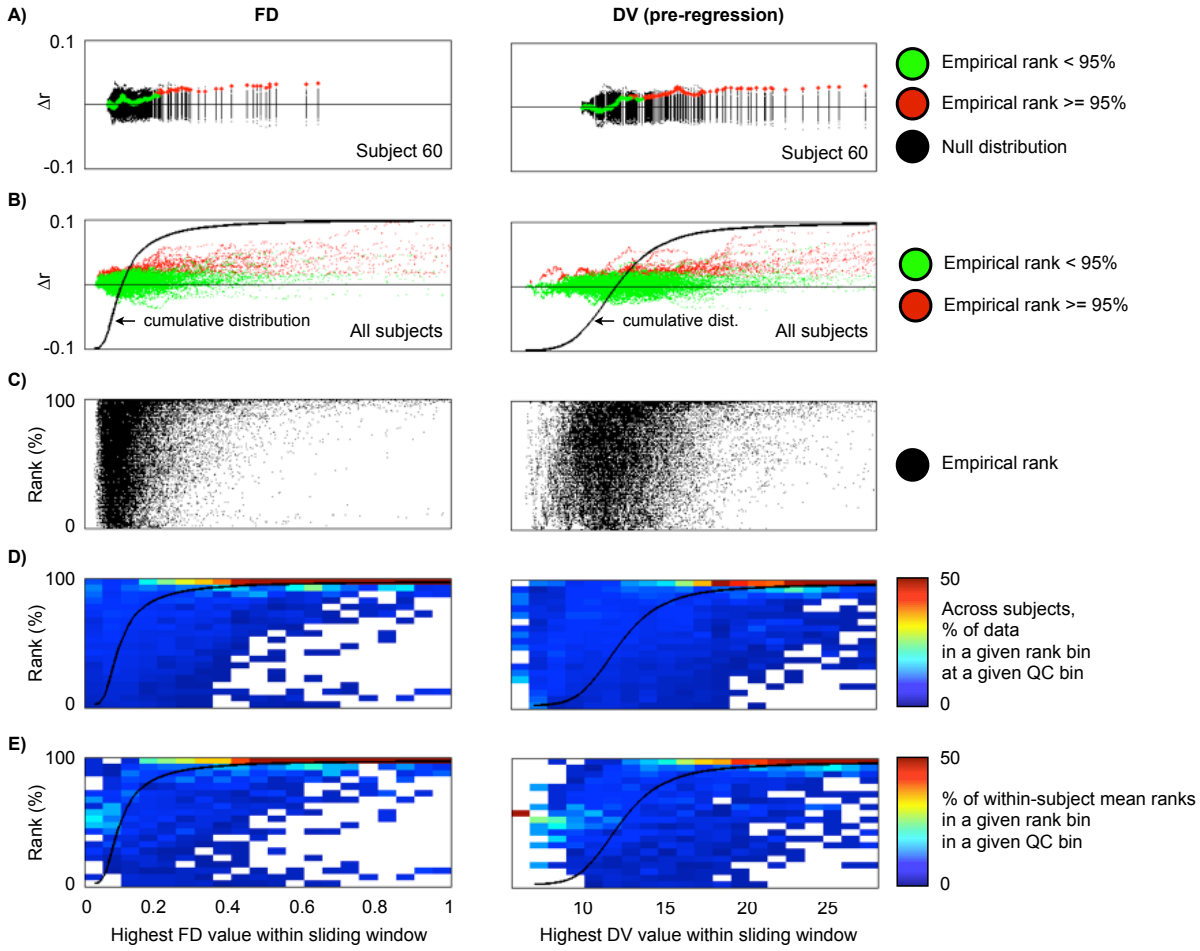

Figure S7: Determining when QC values translate to changes in correlation. A) For a single subject, the within-subject changes in mean short-distance correlation seen in a 50-volume sliding window are shown as a function of the highest FD value found within each window. The black points establish random expectations, and are produced by random orderings of the data. **B)** The changes in correlation produced by QC-ordered data across all subjects. **C)** The empirical ranks of all QC-ordered data from all subjects (~35,000 windows). **D)** A heat map showing the across-subject distribution of empirical ranks within binned QC ranges. Rank bins are 0-100% in 5% bins. With 20 rank bins, 5% of the data should fall in each rank bin by chance. **E)** Within each QC bin, within-subject mean rank is calculated, and the distribution of subject mean ranks in each QC bin is plotted as in (D).

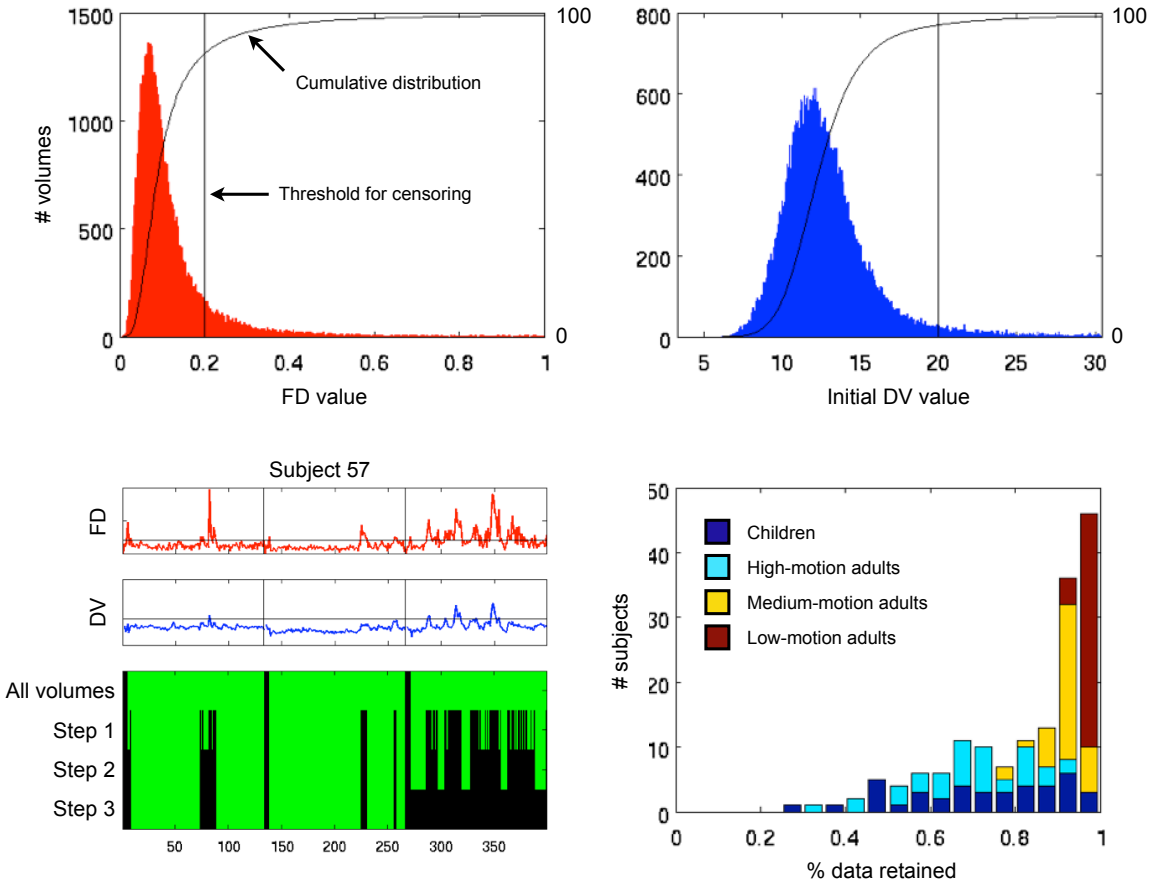

Figure S8: Censoring data for reprocessing. At top, the distribution of FD and initial DV across 160 subjects. A histogram and a cumulative distribution are shown, along with the thresholds selected for reprocessing. At bottom left, for a single subject (one of the 7 subjects who lost a run), the FD and initial DV traces are shown with horizontal lines at the selected thresholds. The 4 temporal masks below show the data qualifying for reprocessing through different steps of mask formation. At bottom right, the distribution of data remaining across the 4 cohorts.

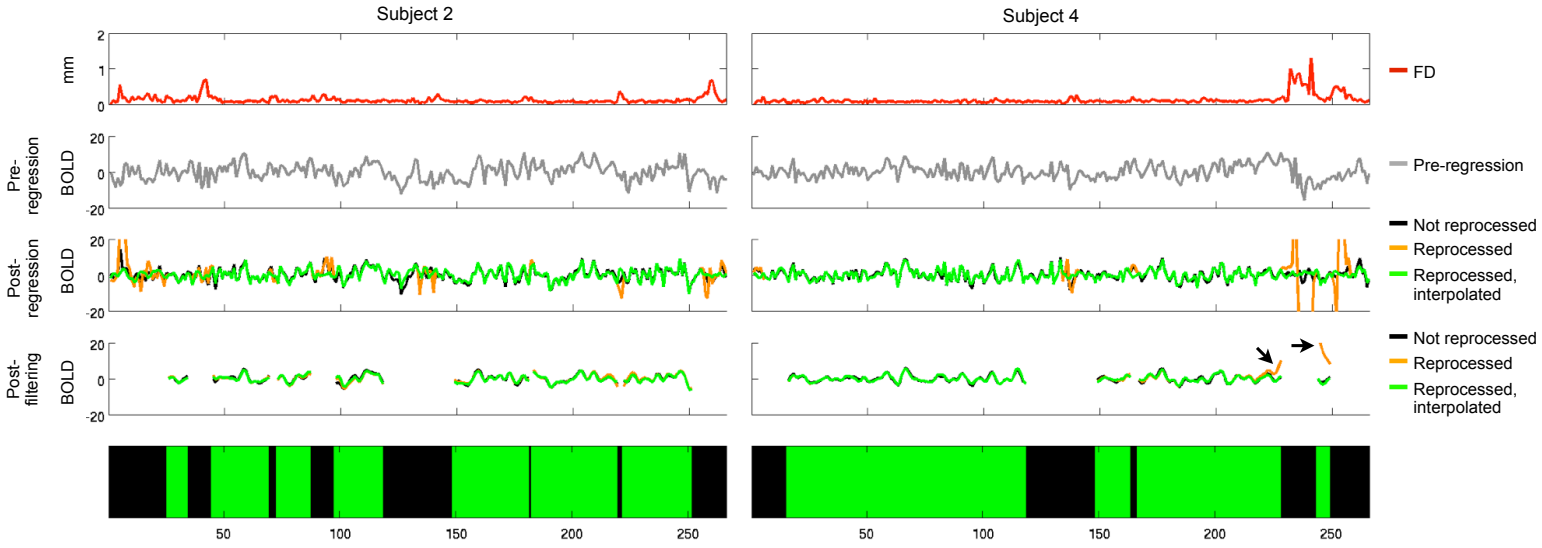

Figure S9: Reprocessing should be accompanied by data replacement. Data from two subjects are shown. At top, the FD trace. Next, a single ROI timeseries is shown, after demeaning and detrending but prior to nuisance regression, then after regression, then after temporal filtering. The final row shows the temporal mask used to reprocess the subject. In the subject at left, reprocessing with or without interpolation produces similar final timeseries (bottom panel). But on the right, the large-amplitude signals during motion contaminate adjacent timepoints when the data are reprocessed without interpolation (the orange deviations indicated by arrows). This occurs because in the 'reprocessed' strategy without interpolation these censored timepoints are neither replaced nor do they contribute to regression fits, and they may therefore contain outlying values that are largely uncorrected by processing and that substantially alter temporally adjacent timepoints during frequency filtering. These data were prepared using regressors [GS GS′ WM WM′ CSF CSF′ R R^2 R_{t-1} R_{t-1}^2].

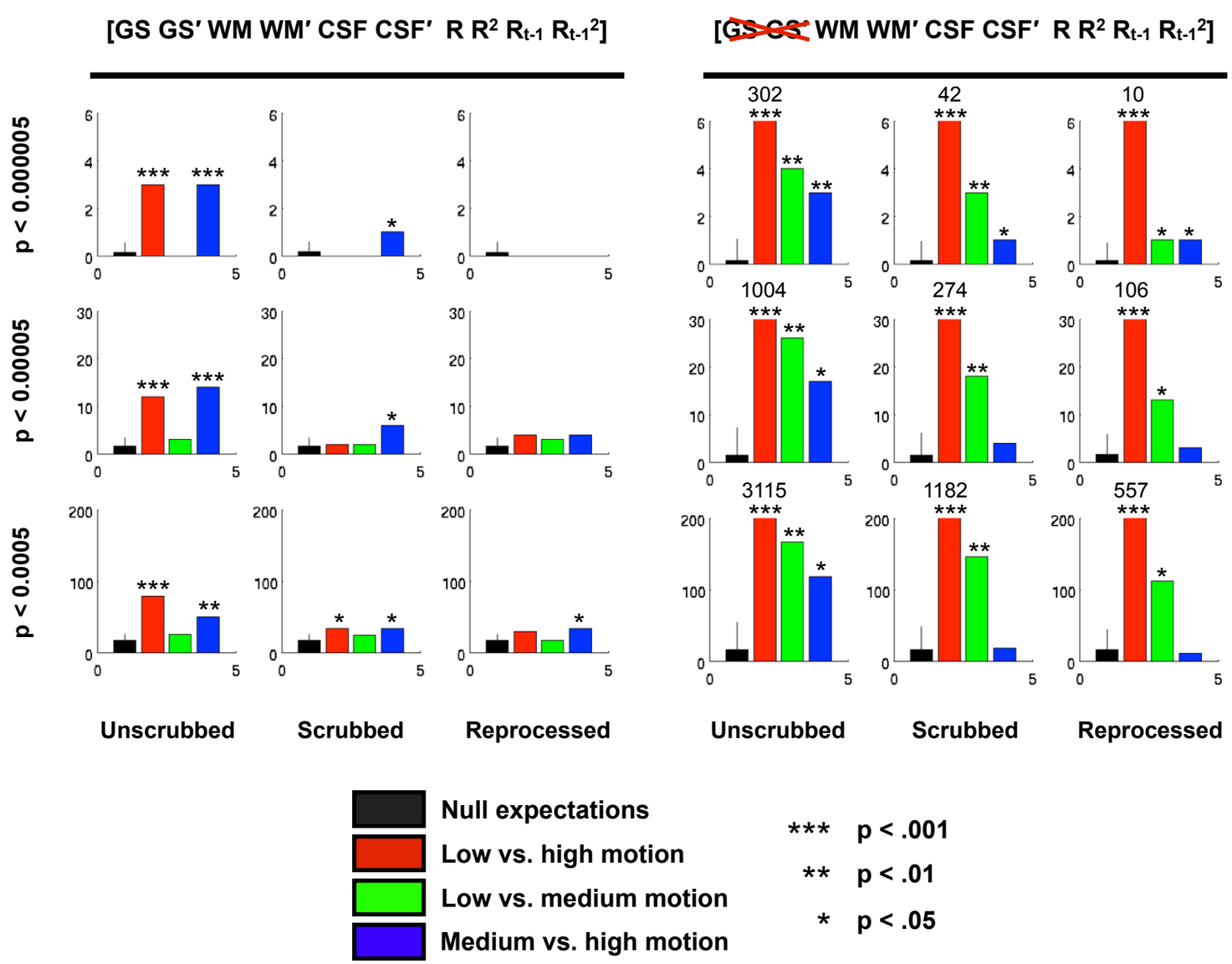

Figure S10: After Figure 13 but for 3 statistical thresholds to define group differences. The data in Figure 13 are the middle row of the plots. Stricter and more lenient thresholds (those used in Figure S5) are in the upper and lower rows.